Origin of anomalous magnetocaloric effect in $(Dy_{1-z}Er_z)Al_2$ alloys

A. L. Lima,[1] I. S. Oliveira,[1] A. M. Gomes,[1] and P. J. von Ranke[2,*]
[1]*Centro Brasileiro de Pesquisas Fisicas, Rua Dr. Xavier Sigaud, 150, Rio de Janeiro 22290-180, Brazil*
[2]*Universidade do Estado do Rio de Janeiro, Rua São Francisco Xavier, 524, Rio de Janeiro 20550-013, Brazil*
(Received 27 February 2002; published 29 April 2002)

We report a theoretical description of the anomalous magnetocaloric peak in $(Dy_{1-z}Er_z)Al_2$ in the concentration range $0.15<z<0.5$ which was experimentally discovered by Gschneidner and co-workers. The anomalous peak was investigated using a Hamiltonian that includes the crystalline electrical field effects.

DOI: 10.1103/PhysRevB.65.172411 PACS number(s): 75.30.Sg, 65.40.−b, 65.40.Gr

We investigated theoretically $(Dy_{1-z}Er_z)Al_2$ alloys that are strong candidates for magnetic refrigerant materials. One of the biggest challenges in the magnetic refrigeration is to find a proper magnetic material to work as a refrigerant material, which must present two fundamental characteristics[1]: (a) large isothermal entropy changes upon variation of the external magnetic field and (b) large temperature change in the adiabatic process. In simple ferromagnetic systems, for instance, $DyAl_2$ and $ErAl_2$, only one peak in the magnetocaloric potential near or at Curie temperature is expected. Recently, it was experimentally observed that $(Dy_{1-z}Er_z)Al_2$ alloys, for concentration varying $0.15<z<0.5$, present two peaks in the adiabatic temperature variation upon the change of the applied magnetic field from zero to 7.5 T. The upper temperature peak is due to ferromagnetic ordering, while the nature of the lower one was not understood.[2] In order to investigate the origin of the second peak, we developed a microscopic model, in which the Hamiltonian is solved exactly, considering the exchange interaction, the crystalline electric field (CEF) and the Zeeman interaction. We determined the adiabatic temperature change vs temperature in $(Dy_{1-z}Er_z)Al_2$ for $z=0.0$, 0.30, 0.5, 1.0. The theoretical results obtained are in good agreement with the experimental measurements and the anomalous peak was fully understood and associated with the high density of CEF levels. The investigation on the microscopic mechanism that is responsible for the large range of temperature variation in a adiabatic process in which refrigeration/heating occurs, can have a high impact on the refrigerant magnetic materials research.[3]

The thermodynamic properties of our interest, in the magnetic system $(Dy_{1-z}Er_z)Al_2$, can be calculated starting from the following Hamiltonian,

$$\hat{H}_{\mathrm{CEF}}=W\left[\frac{X}{F_4}(O_4^0+5O_4^4)+\frac{(1-|X|)}{F_6}(O_6^0-21O_6^4)\right]-g\mu_B H J^z, \tag{1}$$

where the first term describes the single-ion CEF Hamiltonian written in the Lea, Leask, and Wolf (LLW) notation[4] where W gives the CEF energy scale and X $(-1<X<1)$ gives the relative contributions of the fourth and sixth degree in O_n^m Stevens' equivalent operators.[5] The constants F_4 and F_6 have the values $F_4=60$ and $F_6=13862$. The second term is the effective Zeeman interaction in which the exchange interaction was included in molecular field approximation. Here, g is the Lande factor, μ_B is the Bohr magneton and $H=H_0+\lambda M$ is the external magnetic field plus the effective molecular field with the molecular field constant λ, and M is the magnetization, which can be calculated from the self-consistent solution of the magnetic state equation,

$$M=g\mu_B\frac{\Sigma\langle\varepsilon_i|J^z|\varepsilon_i\rangle\exp[-\varepsilon_i/KT]}{\Sigma\exp[-\varepsilon_i/KT]}, \tag{2}$$

where ε_i and $|\varepsilon_i\rangle$ are, respectively, the energy eigenvalues and eigenvectors of Hamiltonian (1).

The three main contributions to the total entropy in the considered magnetic system are

$$S(H,T)=3R\left\{4\left(\frac{T}{\Theta_D}\right)^3\int_0^{\Theta_{D/T}}\frac{x^3dx}{\exp(x)-1}-\ln\left[1-\exp\left(-\frac{\Theta_D}{T}\right)\right]\right\}+\gamma T+R\left[\ln\left[\sum\exp\left(-\frac{\varepsilon_i}{KT}\right)\right]+\frac{\langle E\rangle}{KT}\right], \tag{3}$$

where R is the universal gas constant, Θ_D is the Debye temperature, γ is the electronic heat capacity coefficient and $\langle E\rangle$ is the mean energy. The first and second terms in relation (3) represent the lattice (Debye term) and electronic contribution that are very easy to be calculated since they depend only on temperature. The last term comes from magnetic interaction and besides the temperature, it depends also on $H=H_0+\lambda M$. Therefore, the magnetic entropy term must be calculated in self-consistent way. For a given temperature T and for an external magnetic field H_0, the transcendental equation (2) must be solved in order to obtain the exchange field to update the magnetic entropy.

The adiabatic increase in the sample temperature, $-\Delta T_{\mathrm{ad}}=T_2-T_1$ (the magnetocaloric effect) is theoretically calculated considering the variation of the external magnetic field, from zero to H_0 for instance, and solving the following equation $S(H_0=0,\ T_1)=S(H_0\neq 0,\ T_2)$.

The numerical procedures to treat the model Hamiltonian applied to the magnetic system $(Dy_{1-z}Er_z)Al_2$ is simplified since both Dy and Er have the same total angular momentum, $J=\frac{15}{2}$, leading to the same matrix order for all z concentration. The other magnetic parameters $\{g,\ \lambda,\ W,\ X\}$ were considered to be dependent on concentration. In this

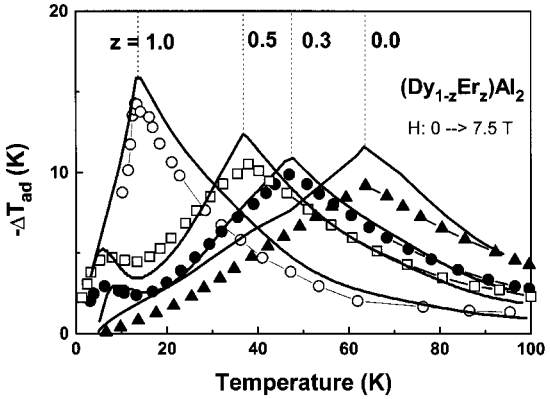

FIG. 1. The $-\Delta T_{\mathrm{ad}}$ vs temperature in $(\mathrm{Dy}_{1-z}\mathrm{Er}_z)\mathrm{Al}_2$ ($z=0$, 0.3, 0.5, 1.0) for a magnetic field change from 0 to 7.5 T. The symbols represent the experimental data and the full curves come from theoretical calculations.

approximation, for a given z ($0 \leqslant z \leqslant 1$) value, the set parameter used in $(\mathrm{Dy}_{1-z}\mathrm{Er}_z)\mathrm{Al}_2$ was $\{g,\ \lambda,\ W,\ X\}^{\mathrm{Dy}_{(1-z)}\mathrm{Er}_{(z)}\mathrm{Al}_2} = z\{g,\ \lambda,\ W,\ X\}^{\mathrm{ErAl}_2} + (1-z)\{g,\ \lambda,\ W,\ X\}^{\mathrm{DyAl}_2}$, where the set parameters for the extreme concentrations are $\{6/5,\ 13.3\ \mathrm{I}^2/\mathrm{meV},\ -0.0252\ \mathrm{meV}, -0.262\}^{\mathrm{ErAl}_2}$ and $\{4/3,\ 44.0\mathrm{I}^2/\mathrm{meV},\ -0.011\ \mathrm{meV}\ ,0.3\}^{\mathrm{DyAl}_2}$, taken from Ref. 6. The effective Debye temperature was taken from the nonmagnetic and isostructural systems LaAl_2 and LuAl_2 using the assumptions considered in Ref. 7; (4) The electronic heat capacity coefficient, $\gamma = 5.5\ \mathrm{mJ\,mol^{-1}\,K^{-2}}$, was assumed to be equal to that of the nonmagnetic compound LuAl_2.[7]

Figure 1 shows the $-\Delta T_{\mathrm{ad}}$ vs temperature in $(\mathrm{Dy}_{1-z}\mathrm{Er}_z)\mathrm{Al}_2$ for ($z=0$, 0.3, 0.5, and 1.0) for magnetic field change from zero to 7.5 T. The symbols represent the experimental data taken from Ref. 2 and the solid curves were calculated from our theoretical model described above. The agreements between theoretical and experimental data is good since no fitting procedure was performed in the model parameters. The main goal of this paper is not to fit a standard model to experimental data, but to understand the nature of the lower anomalous peaks observed experimentally (see in Fig. 1 the curves for $z=0.3$ and $z=0.5$). These lower

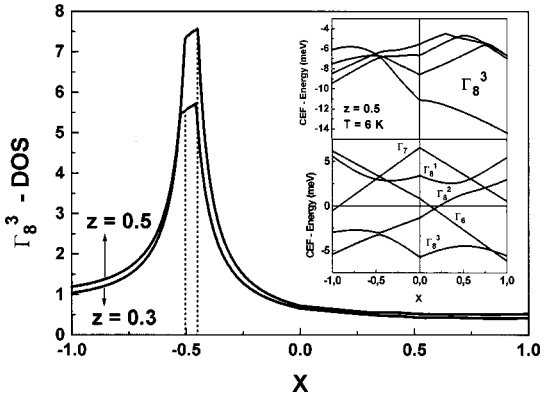

FIG. 2. The Γ_g^3-DOS vs X-CEF parameter calculated for $z=0.3$ and $z=0.5$. The lower inset gives the LLW diagrams and the upper inset shows the splitting of the Γ_g^3 CEF level calculated for $z=0.5$ at $T=6$ K.

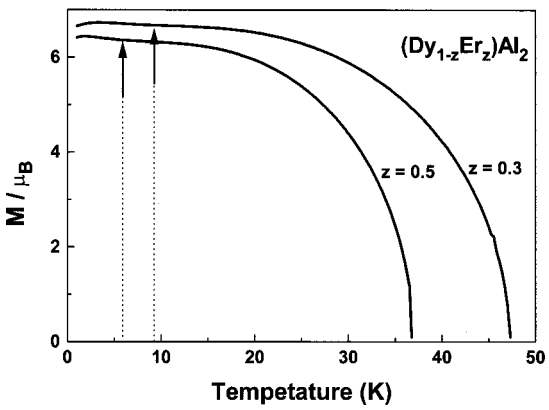

FIG. 3. Theoretical magnetization curves vs temperature in $(\mathrm{Dy}_{1-z}\mathrm{Er}_z)\mathrm{Al}_2$ ($z=0.3$,0.5).

anomalous peaks are not connected to the phase transition as is the case of the higher peaks, which come from ferro-paramagnetic phase transition. The nature of anomalous peak was investigated taking into account the CEF levels scheme using a LLW diagram. This diagram, displayed in the down inset of Fig. 2, can be obtained considering only the energy eigenvalues of the CEF Hamiltonian vs the X-CEF parameter that ranges from $X=-1$ to $X=1$, for a fixed value of W scale. The following set of CEF levels appears: Γ_8^3 (quadruplet), Γ_8^2 (quadruplet), Γ_8^1 (quadruplet), Γ_7 (doublet), and Γ_6 (doublet). The upper inset of Fig. 2 shows only the Γ_8^3 ground state in presence of the molecular field that comes from magnetization for concentration $z=0.5$ at $T=6$ K (in this temperature the anomalous peak appears in $-\Delta T_{\mathrm{ad}}$ vs T, for $z=0.5$, see Fig. 1). The value of the magnetization, responsible for the splitting of the Γ_8^3 ground levels is $M \approx 6.16\mu_B$ and is shown by the left arrow in Fig. 3 that gives the magnetization vs temperature for $Z=0.5$ and $Z=0.3$. Figure 2 shows the density of states (DOS) of the Γ_8^3 level vs X-CEF parameter defined here as $\mathrm{DOS}=4/(E_4-E_1)$, where (E_4-E_1) is the difference between the fourth and ground magnetic energy states. The DOS calculated for $z=0.5$ presents higher value compared with the one for $z=0.3$. It was expected since the experimental data and theoretical predic-

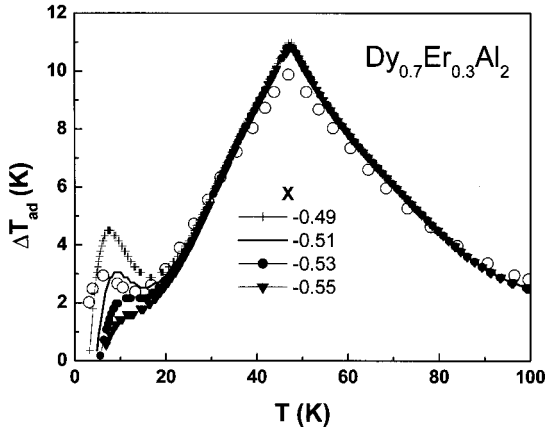

FIG. 4. The influence of the X-CEF parameter on the behavior of the lower peak of the $-\Delta T_{\mathrm{ad}}$ vs temperature curve for $z=0.3$.

tion show the higher anomalous peak in the $-\Delta T_{ad}$ vs T curves for $z=0.5$ (see Fig. 1). In order to confirm our results, we have performed a theoretical investigation in influence of the X parameter in the $-\Delta T_{ad}$ vs T curve for $z=0.3$ (see Fig. 4). As we change the value of X parameter, the intensity of the second peak at $T\sim 6$ K decreases. The highest intensity of the second peak occurs for the value of X parameter for which the DOS of the Γ_8^3 level presents maximum value.

It can be observed, in Fig. 3, the CEF quenching in the magnetization curves. Note that as z increases, the modulus of W-CEF parameter increases and so does the CEF quenching. Also, the critical Curie temperature, calculated using our model, varies linearly with z-concentration and is in excellent agreement with the experimental results.

In general, the best materials to work as a magnetic refrigerant in a magnetic refrigerator are those that supply the maximum amount of cooling over the widest temperature range (tablelike characteristic). In this way, the full theoretical comprehension of the origin of the second peak in $-\Delta T_{ad}$ vs T, that was experimentally observed, can have a high impact on designing new magnetic materials to be used in magnetic refrigeration.

This study was supported by the following Brazilian agencies: CNPq, CAPES, FAPERJ and UERJ.

*Corresponding author. Present address: Universidade do Estado do Rio de Janeiro, Instituto de Física, Rua São Francisco Xavier, 524, Rio de Janeiro 20550-013, Brazil. Email address: vonranke@nitnet.com.br

[1] K. A. Gschneidner, Jr. and V. K. Pecharsky, Annu. Rev. Mater. Sci. **30**, 387 (2000).

[2] K. A. Gschneidner, Jr. and V. K. Pecharsky, and S. K. Malik, Adv. Cryog. Eng. **42**, 475 (1996).

[3] B. J. Korte, V. K. Pecharsky, and K. A. Gschneidner, Jr., Adv. Cryog. Eng. **43**, 1737 (1998).

[4] K. R. Lea, M. J. M. Leask, and W. P. Wolf, J. Phys. Chem. Solids **33**, 1381 (1962).

[5] K. W. H. Stevens, Proc. Phys. Soc., London, Sect. A **65**, 209 (1952).

[6] H. G. Purwins and A. Leson, Adv. Phys. **39**, 309 (1990).

[7] P. J. von Ranke, V. K. Pecharsky, and K. A. Gschneidner, Jr., Phys. Rev. B **58**, 12 110 (1998).